

**Interner Bericht**  
**DESY D3-69/5**  
**Oktober 1969**

**DESY-Bibliothek**

**14. OKT. 1969**

**Radiation Problems Around the DESY 7 GeV Electron Accelerator**

**K. Tesch**

**Deutsches Elektronen-Synchrotron DESY, Hamburg, Germany**

**Invited paper to be presented at the Conference on  
Accelerator Dosimetry and Experience, Stanford,  
November 5-7, 1969**



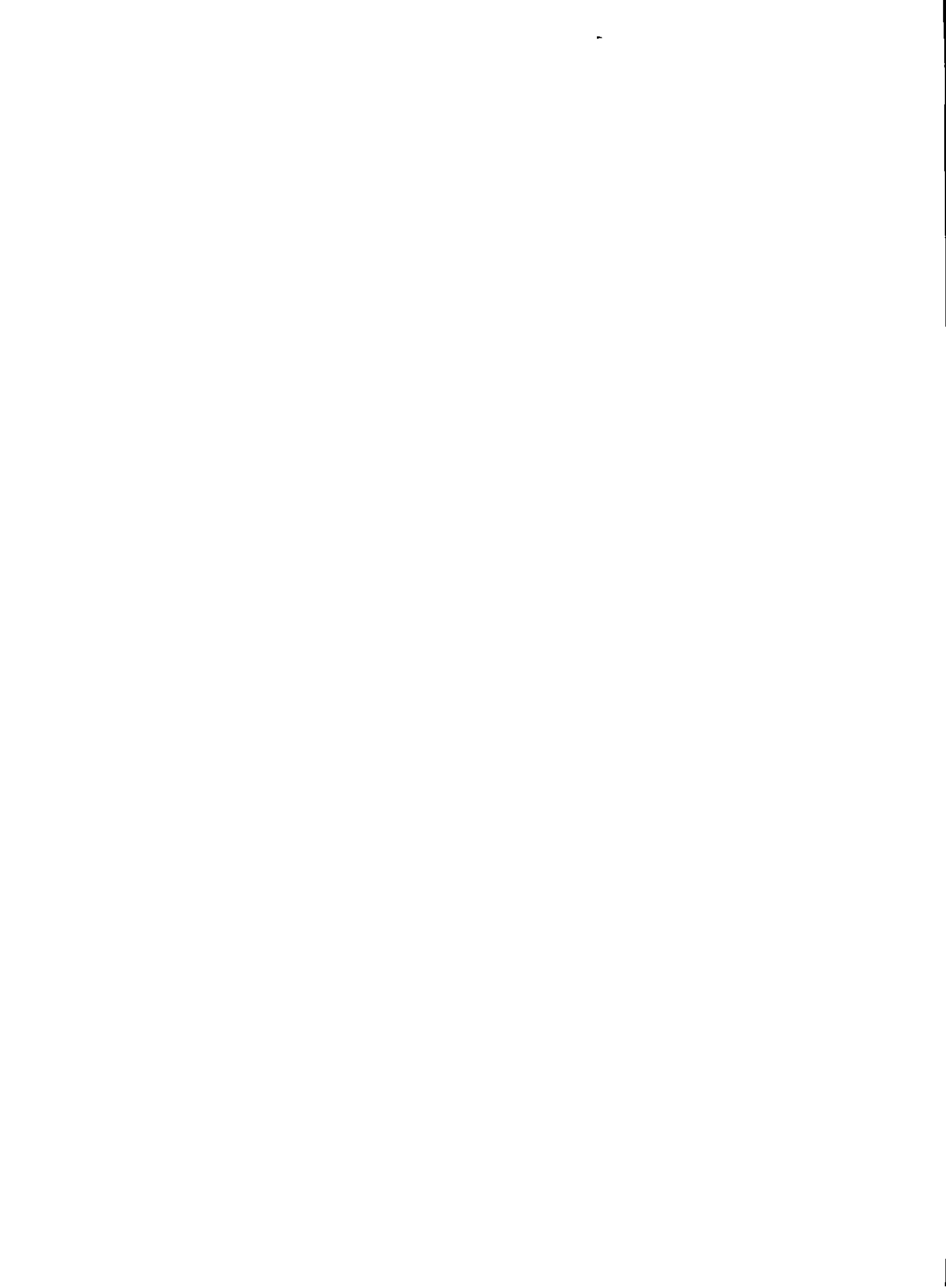
# Radiation problems around the DESY 7 GeV electron accelerator

K. Tesch

Deutsches Elektronen-Synchrotron DESY, Hamburg, Germany

Summary: This paper deals with the dosimetry of the accelerator-produced radiation. First of all, a few data on the accelerator are given. Then the basic concept of our radiation protection measurements is described, which is somewhat different from the measuring methods used at other accelerators. In several experiments done in the past with a quite general experimental set-up we gained enough experience about the radiation field and possible instruments to perform all stray-radiation measurements around the accelerator with simple rem-responding instruments. It is here reported in some detail how this procedure works in practice.

In the second part, two methods are reported which are under development in order to extend the range of our neutron dosimetry to 10 - 100 MeV. According to our concept, rem-responding instruments are wanted. One method combines the detector designed by J.W. Leake with another  $\text{He}^3$ -counter surrounded by an 18" sphere of polyethylene. In addition, a liquid scintillator is tried as a neutron dosimeter; pulses due to electrons are rejected by pulse-shape discrimination.



One of the more important duties of the Radiation Protection Group at every accelerator is the determination of the dose equivalent or of the dose equivalent rate in accessible areas. I will therefore limit myself to this problem and show how such measurements are carried out at DESY and on which concept the measurements are based. In so doing I will deal with one special problem in more detail, namely with the dosimetry of high-energy neutrons above 10 MeV.

First of all here are some data on the accelerator. The electron synchrotron is situated in an underground ring which has a 100 m diameter. The normally reached energy is 7.5 GeV and a typical value for the circulating current is 10 mA. The accelerator is shielded above with sand and towards both experimental halls with movable concrete walls, so that, without external beams, the radiation level outside the machine can be disregarded. Fig. 1 shows one of the experimental halls. Typical values for the flux of an external  $\gamma$ -beam is  $5 \cdot 10^{10}$   $\gamma_{\text{eff}}/\text{s}$ , and for the external electron beam  $5 \cdot 10^{11}$  e/s; the latter has a beam power of 0.5 kW (at 6 GeV). The length of a radiation pulse is approximately 1 ms so that the duty cycle is 0.05 at a repetition rate of 50 cycles/s. The Faraday-cup, respectively the quantameter, in which the beams end, is situated in a concrete house, the rest of the experimental area being surrounded by a 1 m thick heavy concrete wall. In general the area is not shielded in the upper direction.

It is our aim to keep the grounds around the experimental areas freely accessible, and for this reason the radiation level has to be below 0.75 mrem/h on an average. Areas from which one can look down into the experimental areas (e.g. the crane galleries) are considered as controlled areas.

In the above-mentioned areas the dose equivalent rate has to be measured regularly. The following radiation components are to be expected: In the direction of the beam the electromagnetic cascade and muons as penetrating components; low energy electrons and photons which are scattered outside the experimental areas; neutrons both as penetrating component and as scattered radiation. The main part of the neutrons are composed of giant - resonance neutrons with a mean energy of 1 MeV; the more energetic neutrons are produced in the nucleus by pseudodeuteron disintegration and pionic effects.

There are several possibilities for estimating the dose equivalent rate in such a mixed radiation field. The most comprehensive method (see, e.g. Reference 1) is the following: the flux density and energy distribution of each component of the field are measured with many instruments. The dose equivalent rates of the individual components are calculated from this and then added together. This method is used at many large accelerator centers; the used instruments are various ionization chambers, activation probes,  $\text{BF}_3$ - and

recoil counters, nuclear emulsions, moderated counters for thermal neutrons etc. Obviously this method gives the most comprehensive information on the radiation field from which further improvements of the shielding can easily be derived if necessary. The costs for instruments and working time are, however, considerable. Another point is the following: it is certainly possible to describe the radiation field in physical terms with some effort. The great uncertainty, however, then lies in the calculation of the biological terms from the physical ones, or in the change from flux density to dose equivalent rate, or in the uncertainty of the quality factor. The concept of the rem is only a very rough approximation, the effect of the radiation field on the human body is much too complex to be described with only one single number. The errors of the quality factors are by and large unknown and this uncertainty reduces the advantage of a comprehensive determination of the physical data of the radiation field.

A method requiring less effort is the simultaneous measuring of the dose rate (in rad/h) with a tissue-equivalent ionization chamber and of the mean quality factor. However, apart from the experimental difficulties of a determination of a mean quality factor this gives no information, apart from the radiological data, on the radiation field.

At DESY we have tried to carry out the routine radiation protection measurements as simply as possible with a minimum of instruments and working time, without any loss to security, and in so doing to obtain additional informations from which, for example, shielding deficiencies can be recognized and improved. In the past years we had the possibility to study the individual radiation components in several experiments. This involved shielding experiments, electromagnetic cascade measurements, measurements of neutron production rates, sky-shine measurements, dose measurements in primary beams. These are all carried out with very different measuring methods. The results have been published<sup>2</sup> and are not going to be repeated here. On the one hand, they serve for carrying out simple shielding calculations, and on the other hand, they show that it is possible to carry out the radiation protection measurements around the accelerator with only two simple portable instruments which are directly calibrated in rem/h. These are the well-known Jordan Survey Meter<sup>+</sup>), a Neher-White ionization Chamber filled with argon, and the Neutron Rem Counter<sup>++</sup>) which was developed by Andersson and Braun<sup>3</sup>.

The Jordan Chamber serves for measuring the dose rate of the electromagnetic components and the muons. For this the following properties are necessary:

---

+) The Victoreen Instruments Co., Cleveland, Ohio

++) Aktiebolaget Atomenergi, Stockholm, Sweden, and other firms

1. Insensitivity to neutrons. This is the case because of their construction (steel chamber filled with argon).
2. Correct reading in a pulsed radiation field. We found that even with a duty-cycle of  $1 \cdot 10^{-4}$  up to a mean dose rate of 250 mrad/h no deviation from the saturation current occurred.
3. The calibration of the chamber, which initially was only valid for photons in the energy interval between 0.08 and 1 MeV, should also be correct in the radiation field which surrounds a high-energy  $\gamma$ - or electron beam.

The last point is not trivial and should be explained in more detail: It is well known that a tissue-equivalent ionization chamber (TE chamber) records correctly the dose rate for all types of radiation and energies. We have therefore compared the reading of the Jordan Chamber with that of the TE chamber (wall thickness  $700 \text{ mg/cm}^2$ ) and with the information from an ionization chamber filled with air; the latter has a large thin entrance window ( $3 \text{ mg/cm}^2$ ) which can be closed with a plastic disc having a  $450 \text{ mg/cm}^2$  thickness. This chamber is manufactured by the firm EKCO<sup>+</sup>). The measuring positions were distributed in the experimental halls on the ground and on the crane galleries around the experimental areas, where electron- or  $\gamma$ -beam experiments were set up. The ratios of the dose rates are put together in Table I. The given errors resulted from the averaging over the results from the different positions. As can be seen, the different types of chambers are in good agreement in the measurements around  $\gamma$ -beam areas. Around the electron-beam areas a scattered radiation of charged low-energy particles was seen which caused the measured dose to be heavily dependent on the thickness of the chamber wall. The surface dose as measured with the air chamber can amount to two or three times the dose which was measured with the TE chamber. We decided, however, not to base our evaluation of the radiation level in accessible areas on the surface dose thus measured but to look on the results of the TE chamber as the "standard" dose rate. Then, however, the simple Jordan Chamber is a useful instrument, an underestimate of 20 % for the dose rate is tolerable.

The dose rate of the neutron component is also measured only with a simple portable commercial instrument in routine radiation protection measurements. The instrument in question is the Neutron Rem Counter developed by Andersson and Braun<sup>3</sup>. It comprises a  $\text{BF}_3$ -counter which is surrounded by a special moderator so that<sup>3</sup> the reading can be calibrated in rem/h. The recommendations of the ICRP<sup>4</sup> are the basis for the calculation of the dose equivalent rate from the neutron flux density. For all practical cases the instrument is insensitive to photons and even in pulsed radiation fields it gives correct results.

---

+ ) EKCO Electronics, Southend-on-Sea, Essex, England

In its whole energy range (thermal energy up to 10 MeV) the deviations of its sensitivity curve from that of an "ideal" counter (as recommended by the ICRP) is less than 50 %. In the range 0.03 to 10 MeV the deviations are less than 20 %, which, in view of the already mentioned uncertainty of the quality factor, is more than sufficient. The largest part of the neutron component is recorded by this instrument because about 90 % of the photoproduced neutrons are giant-resonance neutrons and effects such as backward scattering and sky-shine are specially effective in the case of these low-energy neutrons.

However, an upper limit of 10 MeV for the neutron dosimetry is somewhat low a priori. One should at least make sure that higher energies play no role in the scattered radiation; furthermore, simple calculations show that behind insufficient shielding high-energy neutrons are the main component. Our aim was, therefore, to extend the energy range of our neutron dosimetry by a factor of 10.

What other methods are there in the range 10 to 100 MeV? The most common is the activation of a plastic scintillator by the reaction  $C^{12}(n,2n)C^{11}$ . The reaction threshold is 20 MeV. This method, however, gives no unique results around electron accelerators because the reaction  $C^{12}(\gamma,n)C^{11}$  cannot be separated. Besides, an activation method which gives a half-life of 20 minutes is somewhat inconvenient for survey purposes. Other activation methods make use of the production of  $Be^7$  from light nuclei; also Bi-fission-chambers are in use. These reactions have a threshold of approximately 50 MeV, the cross-section then increases up to 100 MeV so that these methods are not very suitable for determining the flux density or dose rate in the energy range already mentioned. Moreover, the sensitivity is low. What we really want for survey purposes in accessible areas is an instrument which gives the dose equivalent rate directly with high sensitivity.

What should the response curve of such an instrument look like? The relation between neutron flux density and dose equivalent rate has been calculated by several authors. Shaw et al.<sup>5</sup> have compiled the results, and from this compilation Fig. 2 has been taken. It shows the neutron flux density which produces 1 mrem/h as a function of the energy and for different depths of tissue. (The results from Neary and Mulvey<sup>6</sup> are also given as a comparison. It is assumed here that the high-energy neutrons are in equilibrium with low energy neutrons after having passed through thick shielding; we use this curve for shielding calculations.) In order to convert flux density into dose equivalent rate one would actually have to take the envelope of these curves, i.e. for each neutron energy that depth of tissue at which the dose is highest. On the other hand, Shaw et al.<sup>7</sup> have shown



that for all practical cases with irradiation from all sides the spectrum of the neutrons does not change much when passing through the human body so that the curve for the surface dose is a better approximation than the envelope. The efficiency of our neutron dosimeter should therefore be constant between 10 and 50 MeV and then up to 100 MeV decrease by approximately 25 %.

A possibility for realising such an instrument is a simple extension of the multi-sphere method which is known for quite a time in the dosimetry of low-energy neutrons. Bonner et al.<sup>8</sup> have first calculated and measured the sensitivity of instruments which consist of a polyethylene sphere with a  $\text{Li}^6$  I-crystal in the middle for detecting thermal neutrons. Desired response curves can be obtained by varying the spheres' diameter and by combining different spheres<sup>9</sup>. In order to keep the instrumental effort as low as possible we proceeded in the following way. A useful instrument for dosimetry up to 10 MeV is the detector developed by Leake<sup>10</sup>. Its advantage is the following: the neutrons slowed down by a special light-weight spherical moderator are detected by a small spherical proportional counter filled with  $\text{He}^3$ . This counter, when correctly biased, is insensitive to  $\gamma$ -radiation as long as pile-up effects are avoided. The normally used  $\text{Li}^6$  I-crystal is sensitive to  $\gamma$ -radiation above 3 MeV, which in fact may lead to erroneous measurements at reactors<sup>10</sup> and even more so at electron accelerators. This instrument, which is anyway available for neutron dosimetry up to 10 MeV, is combined with an 18" diameter polyethylene sphere which is also supplied with a  $\text{He}^3$ -counter. Fig. 3 shows the sensitivity of both instruments as well as that of their combination as a function of the neutron energy, the sensitivity is expressed in pulses /s per 1 mrem/h. The sensitivity of an 18" sphere, expressed in pulses/s per unit of flux density, has been calculated by McGuire<sup>11</sup>. An ideal instrument would give a constant in our plot. As can be seen the deviations from the mean value between 1 eV and 100 MeV are smaller than  $\pm 50$  % and even smaller for a continuous neutron spectrum. The mean sensitivity is 0.60 pulses/s per 1 mrem/h. This combination is, therefore, suitable for the above-mentioned purpose and unique results are obtained because it is insensitive to all other kinds of radiation. Similar results are obtained by combining the Rem Counter developed by Andersson and Braun with an 18" sphere.

A second method for dosimetry of high-energy neutrons gives a sensitivity 10 times higher and with a better response curve. The most simple and also most sensitive way of measuring high-energy neutrons is the use of a plastic scintillator. How does the efficiency of such a scintillator between 10 and 100 MeV look? A computer program for calculating the efficiency, taking into account the carbon atoms in the scintillator, was written by Kurz<sup>12</sup> and improved at DESY by Geweniger<sup>13</sup>.

Fig. 4 shows the results for the liquid scintillator NE 213<sup>+</sup>), 4.7 cm Ø x 4.7 cm long, when pulses above a threshold of 0.5 MeV electron energy are counted. The contributions of the different reactions are here given:

1. Elastic scattering on hydrogen
2.  $C^{12} (n, \alpha) Be^9$
3.  $C^{12} (n, n') 3\alpha$
4.  $C^{12} (n, p xn) + C^{12} (n, d xn)$
5.  $\gamma$ -interaction after the reaction  $C^{12} (n, n') C^{12} \#$
6. Reaction 1 to 4 after reaction 1, should the latter have given a pulse below the threshold
7. Reaction 1 to 4 after an elastic scattering on carbon
8. Reaction 1 to 4 after reaction 3, should the latter have given a pulse below the threshold.

Fig. 5 shows the total efficiency at higher thresholds (expressed in electron energy). A 4 MeV threshold is equivalent to a proton energy of 8.5 MeV. As can be seen the desired efficiency curve can be well obtained at a 4 MeV threshold; a plastic scintillator is therefore in principle an ideal neutron dosimeter.

The difficulty is, of course, to reject pulses which are due to other radiation components. Pulse-shape discrimination was therefore used and a coincidence between the output of the pulse-shape discriminator and the threshold discriminator was required. The method of pulse-form discrimination is well known in nuclear physics but is rarely applied in high-energy physics, because long pulse intervals ( $\sim 200$  ns) are necessary. It is based on the following: the pulse of an organic scintillator is composed of several components, among which usually only the fast component with a decay time of roughly 3 ns is observed. In the case of some special scintillators a slow component with a decay time of 100 to 300 ns can also easily be observed; its amplitude is approximately 3 % of the amplitude of the fast component. The ratio of both components depends, however, on the stopping power of the ionizing radiation, so that  $\alpha$ -particles and low-energy protons can be distinguished from electrons by means of a suitable circuit. During the last few years a larger amount of circuits have been developed for this purpose; they usually aim at trying to separate neutrons of the lowest possible energies from photons. We do not have this problem because a threshold of 8.5 MeV proton energy is applied anyway. For us it is more important that the circuit works at the highest possible  $\gamma$ -rate. I have therefore used a circuit developed by Daehnick and Sherr<sup>14</sup>, which is also built in into a commercial pulse-form discrimination probe<sup>+</sup>).

---

<sup>+</sup>) Nuclear Enterprises, Edinburgh, Scotland

The pulse form discriminator has little influence on the scintillator's efficiency. At neutron energies below 100 MeV the reaction products from carbon reactions are low-energetic enough to be detected by the pulse-form discriminator. The protons from the scattering on hydrogen have, however, at higher energies too small a stopping power and are thus not counted. Fig. 6 shows this effect; it was here assumed that protons with a higher energy than 50 MeV became lost. Furthermore, the influence of edge effects is given which plays a role in the case of such a small scintillator. The resulting response curve is still very suitable for our purpose. Fig. 7 shows the resulting sensitivity curve. The mean value is 6.0 pulses/s per 1 mrem/h, the deviations being smaller than  $\pm 15\%$ .

There are several effects by means of which  $\gamma$ -pulses are counted as neutron-pulses. However, I will not go further into technical details, but instead I would like to mention two other points. The background of the described apparatus is  $4 \cdot 10^{-3}$  pulses/s. According to Hess et al.<sup>15</sup> the flux density of cosmic neutrons between 10 and 100 MeV is approximately  $4 \cdot 10^{-3} \text{ cm}^{-2} \text{ s}^{-1}$ , from which a counting rate of  $3 \cdot 10^{-3} \text{ s}^{-1}$  would be expected. Therefore it can be concluded that the instrument only counted cosmic neutrons and the other components (air shower and muons) were suppressed. Even very large electron- or muon pulses, which may give an incorrect neutron signal as a result of a small nonlinearity of the photomultiplier, cause no difficulties. The high sensitivity of the apparatus is also noticeable: the measured dose equivalent rate of the cosmic neutrons in the energy range mentioned is 0.5  $\mu\text{rem/h}$ .

The main disadvantage of the described method is that the pulse-form discriminator fails in the case of higher  $\gamma$ -rates. Pile-up effects during the decay time of the slow component give false neutron signals. To see if such effects already play a role one should measure the total pulse rate (above 0.1 MeV) and the pulse rate above 4 MeV simultaneously, and then calculate the pile-up effects under an assumption of a 100 - 200 ns pulse duration and with the known duty-cycle of the radiation field. We found that with the duty-cycle of our accelerator ( $\sim 0.05$ ) fields of electromagnetic radiation up to 10 mrem/h caused no difficulties. Here the scintillator was surrounded by 10 mm lead.

Both methods were only recently developed and therefore I am still unable to submit comprehensive results. The following has been found as a result of preliminary measurements with the pulse-form discrimination probe: the ratio of the dose equivalent rate of neutrons above 10 MeV to that of neutrons below 10 MeV is only a few per cent on the floor around the experimental areas, on the crane galleries 10 - 15 %. The value can of course rise to 1 and more behind insufficient shielding. Should these values be confirmed in later measurements, then the component of neutrons above 10 MeV can be disregarded further in the routine radiation protection measurements, and both previously mentioned portable instruments, calibrated in rem/h, are sufficient.

Table 1. Ratio of readings of different ionization chambers

Beam	Location	<u>TE chamber</u> Jordan chamber	<u>EKCO chamber</u> Jordan chamber	
			EKCO window 450 mg/cm <sup>2</sup>	EKCO window 3 mg/cm <sup>2</sup>
γ	Floor and crane galleries	1.0 ± 0.2	1.0 ± 0.1	1.1 ± 0.1
e	Floor	1.2 ± 0.15	2.0 ± 0.5	2.7 ± 0.6
e	crane galleries	1.2 ± 0.25	1.4 ± 0.2	1.4 ± 0.25

## References

1. H.W. Patterson, Accuracy of very-high radiation monitoring, in Radiation Dose Measurements, Stockholm, June 12-16, 1967, European Nuclear Energy Agency, Paris, pp. 459-469, 1967
2. G. Bathow, E. Freytag and K. Tesch, Shielding measurements on 4.8 GeV Bremsstrahlung, Nuclear Instr. Meth. 33: 261 (1965); Shielding of high-energy electrons: the neutron and muon components, Nuclear Instr. Meth. 51: 56 (1967); Measurements on 6.3 GeV electromagnetic cascades and cascade-produced neutrons, Nucl. Physics B 2: 669 (1967); G. Bathow, E. Freytag, U. Clausen and K. Tesch, Skyshine-Messungen und ihr Vergleich mit Abschätzungen aus der Diffusionstheorie, Nukleonik 9: 14 (1967); K. Tesch, Dosisleistung und Toleranzflußdichte hochenergetischer Elektronen- und Gammastrahlen, Nukleonik 8: 264 (1966); G. Bathow, E. Freytag, R. Kajikawa, M. Köbberling and K. Tesch, Measurements of the longitudinal and lateral development of electromagnetic cascades at 6 GeV, presented at this conference.
3. I.Ö. Andersson and J. Braun, A neutron rem counter, Report AE-132, Aktiebolaget Atomenergi, Stockholm, January 1964
4. Recommendations of the International Commission on Radiological Protection, ICRP Publication 4, Pergamon Press, 1964
5. K.B. Shaw, G.R. Stevenson and R.H. Thomas, Depth dose and depth dose equivalent data as functions of neutron energy, Report RHEL/M 149, Rutherford High Energy Laboratory, Chilton, September 1968
6. G.J. Neary and J. Mulvey, Maximum permissible fluxes of high energy neutrons and protons in the range 40 - 1000 MeV, see reference 4
7. K.B. Shaw, G.R. Stevenson and R.H. Thomas, Evaluation of dose equivalent from neutron energy spectra, Health Physics 17: 459 (1969)
8. R.L. Bramblett, R.I. Ewing and T.W. Bonner, A new type of neutron spectrometer, Nucl. Instr. Meth. 9: 1 (1960)
9. D. Nachtigall and F. Rohloff, Verfahren zur Messung der Flußdichte und Dosisleistungsäquivalente von Neutronen im Energiebereich zwischen thermischer Energie und 50 MeV, Nucl. Instr. Meth. 50: 137 (1967)
10. J.W. Leake, A spherical dose equivalent neutron detector, Nucl. Instr. Meth. 45: 151 (1966) and 63: 329 (1968)
11. S.A. McGuire, A dose monitoring instrument for neutrons from thermal to 100 MeV, Report LA-3435, Los Alamos, New Mexico, August 1965

12. R.J. Kurz, A Fortran II program to compute the neutron detection efficiency of plastic scintillator for neutron energies from 1 to 300 MeV, Report UCRL-11339, Lawrence Radiation Laboratory, Berkeley, March 1964 and errata, February 1965
13. Ch. Geweniger, DESY, Hamburg, Diplomarbeit (unpublished), 1969
14. W. Daehnick and R. Sherr, Pulse shape discrimination in Stilbene scintillators, Rev.Sci.Instr. 32: 666 (1961)
15. W.N. Hess, H.W. Patterson, R. Wallace and E.L. Chupp, Cosmic-ray neutron energy spectrum, Phys.Rev. 116: 445 (1959)

Figure captions

- Fig. 1 Map of an experimental hall at DESY
- Fig. 2 Neutron flux densities producing 1 mrem/h vs. neutron energy, for three depths of tissue. The dashed curve shows the calculations of Neary and Mulvey.
- Fig. 3 Sensitivity curves: a) Neutron Dose Equivalent Detector (J.W. Leake), its mean sensitivity of 3.2 pulses/s per 1 mrem/h is divided by 10. b) 18" polyethylene sphere. c) sum of a) and b).
- Fig. 4 Neutron detection efficiency of a liquid scintillator, 4.7 cm  $\emptyset$  x 4.7 cm, threshold 0.5 MeV electron energy. The different contributing reactions are explained in the text.
- Fig. 5 Neutron detection efficiency of a liquid scintillator, 4.7 cm  $\emptyset$  x 4.7 cm, with thresholds of 2, 3, 4, and 5 MeV electron energy.
- Fig. 6 Neutron detection efficiency of a liquid scintillator, 4.7 cm  $\emptyset$  x 4.7 cm, threshold 4 MeV electron energy. The effect of the pulse-shape discrimination and edge effects are shown.
- Fig. 7 Sensitivity calculated from fig. 6

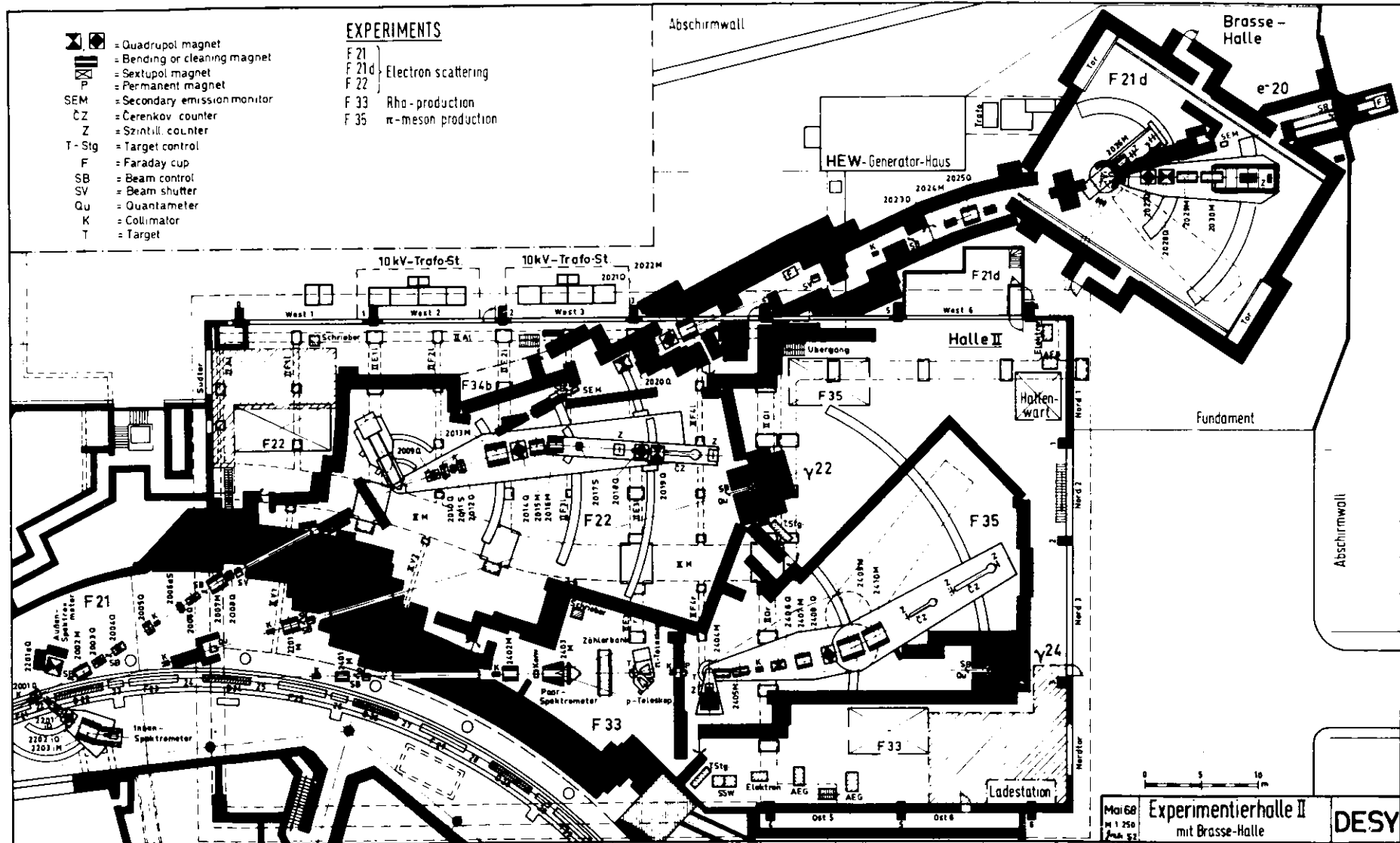


Fig.1



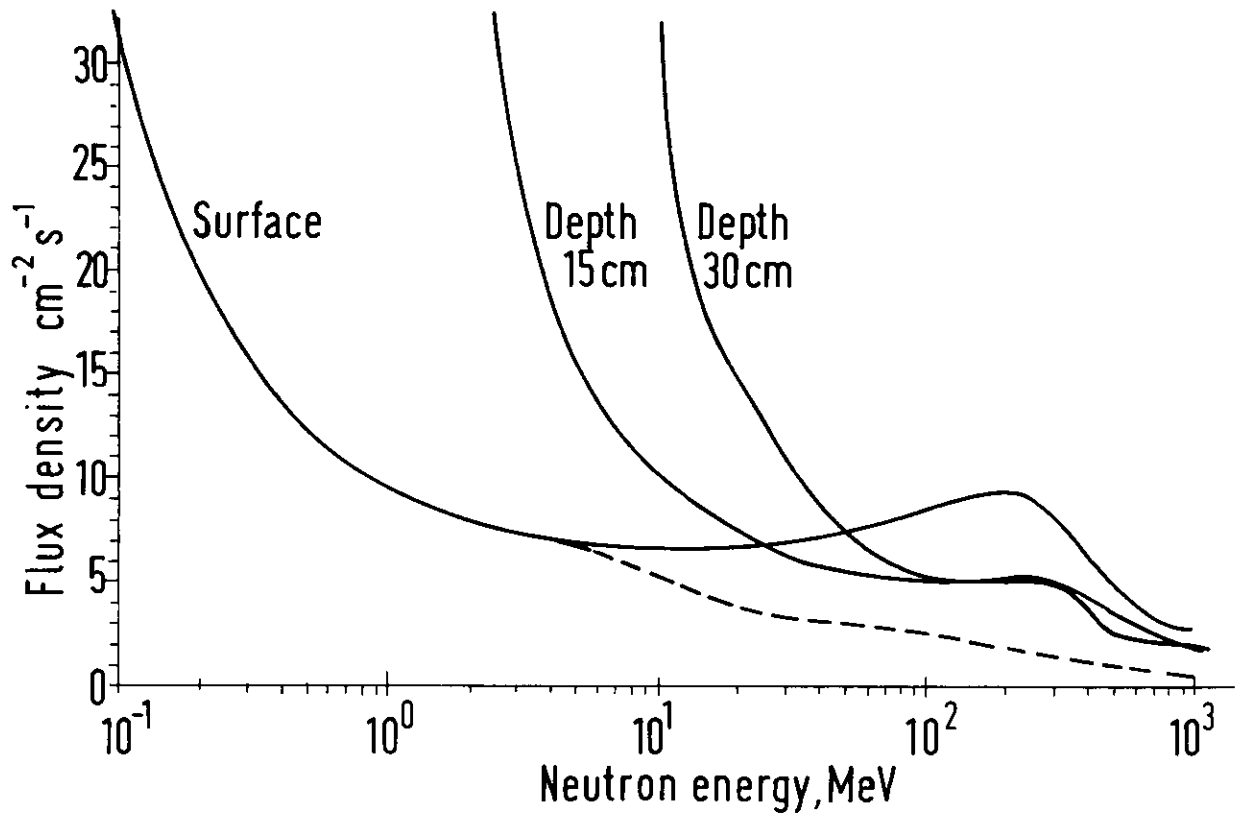


Fig. 2

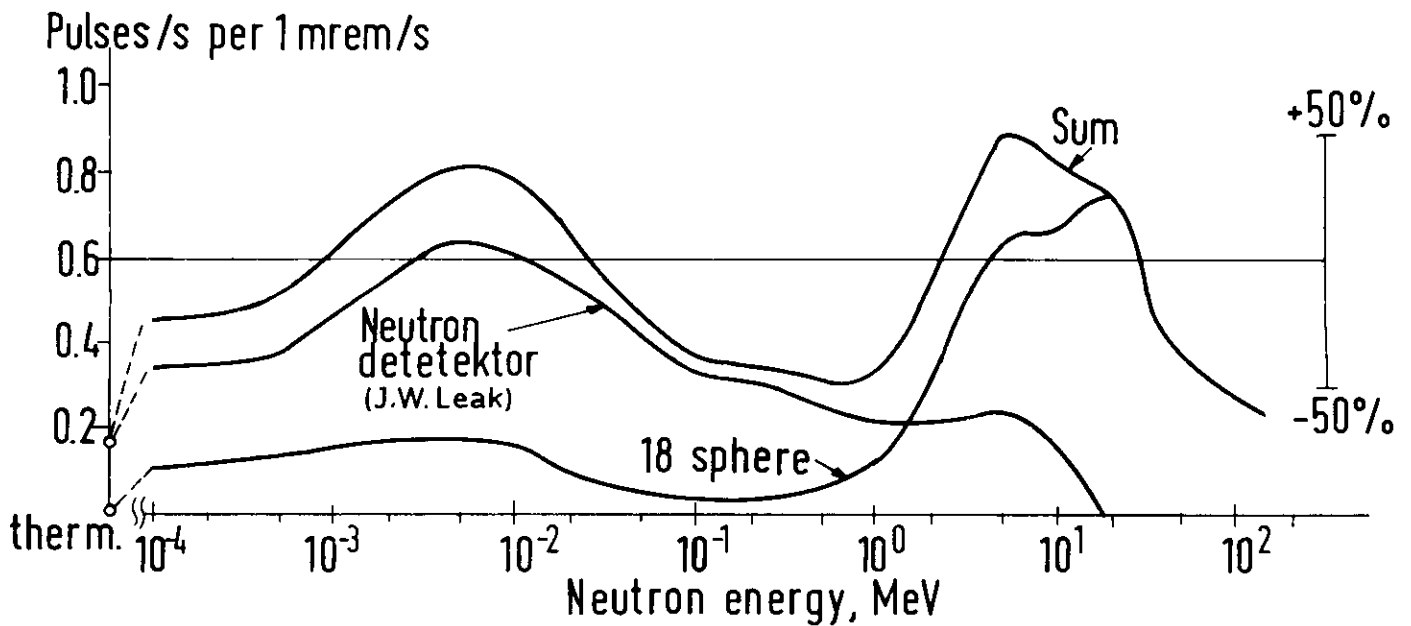


Fig. 3

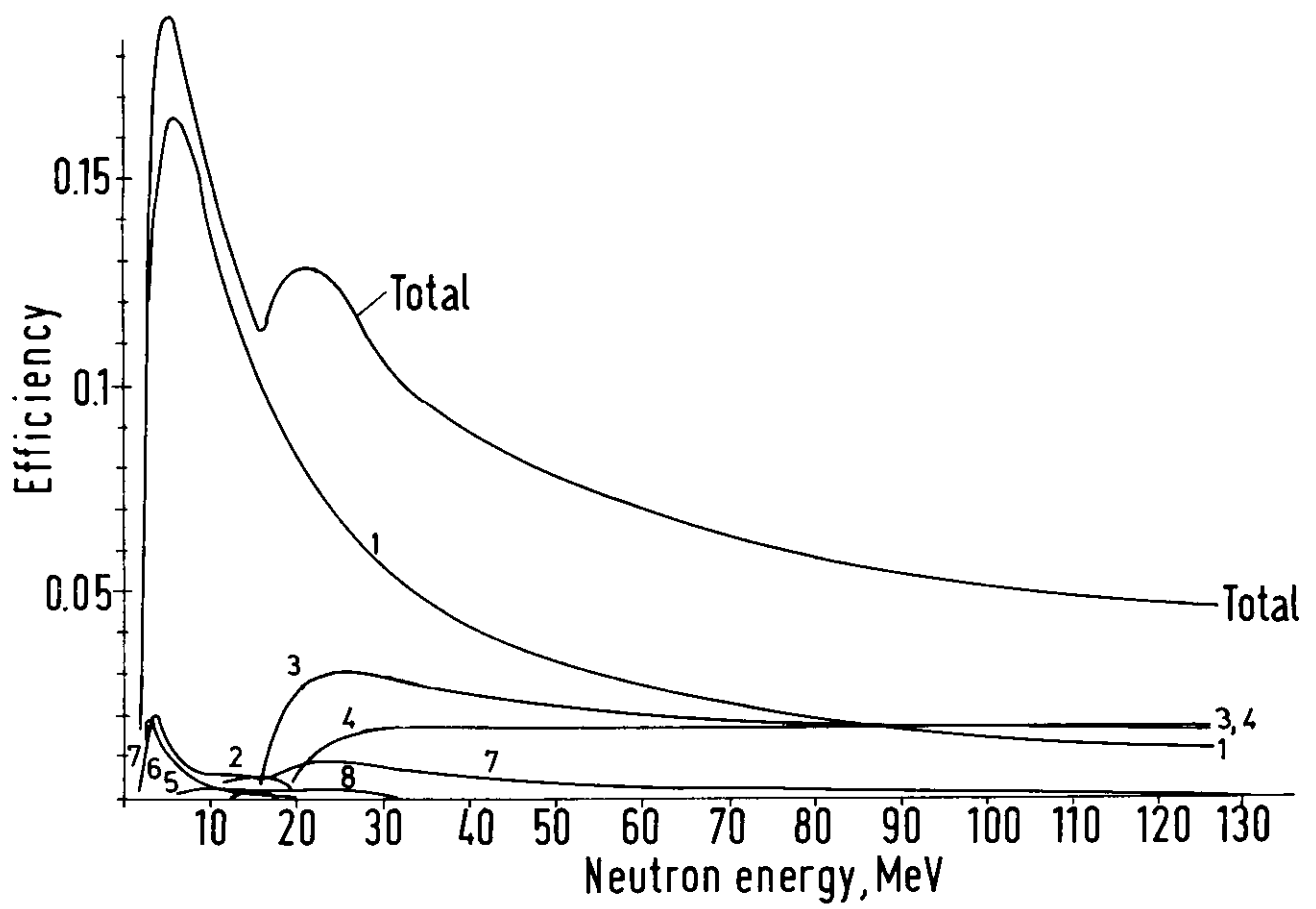


Fig. 4

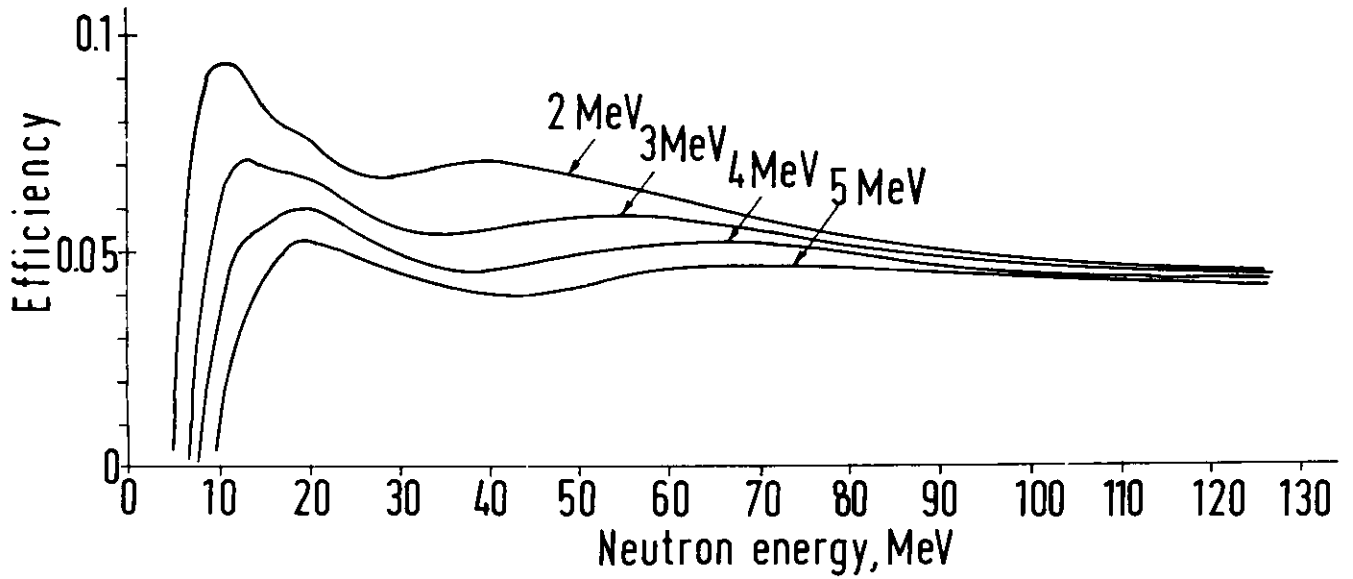


Fig. 5

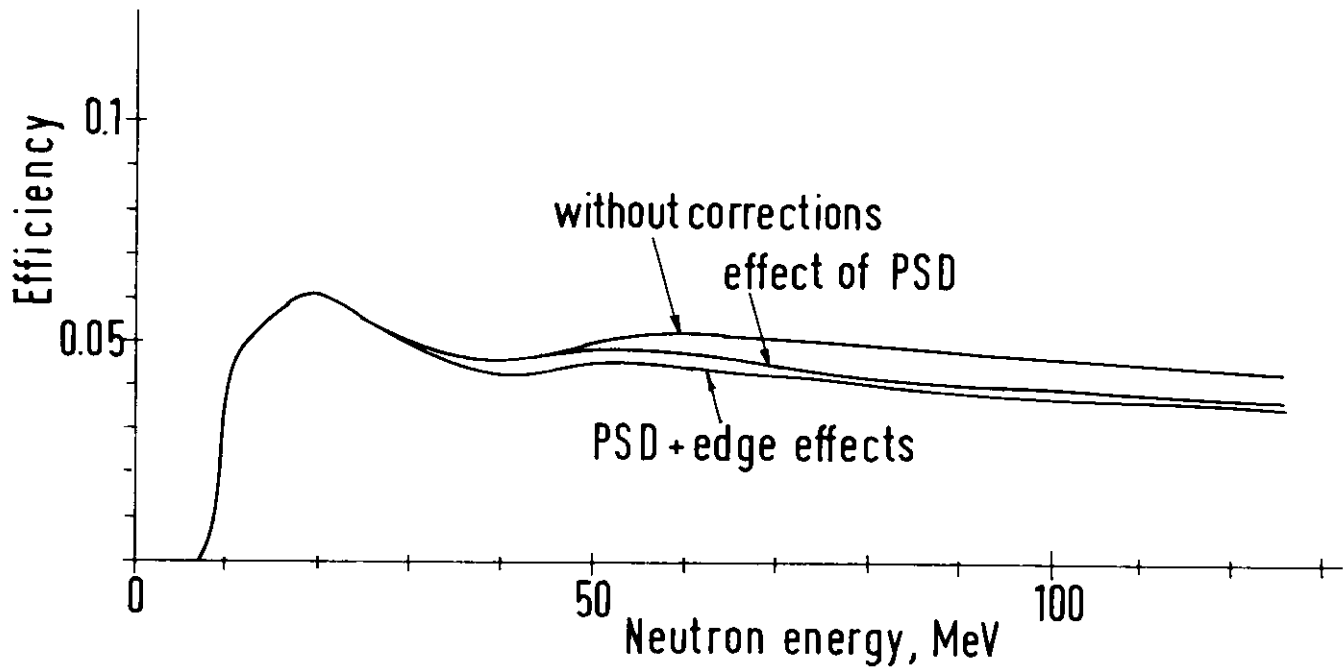


Fig. 6

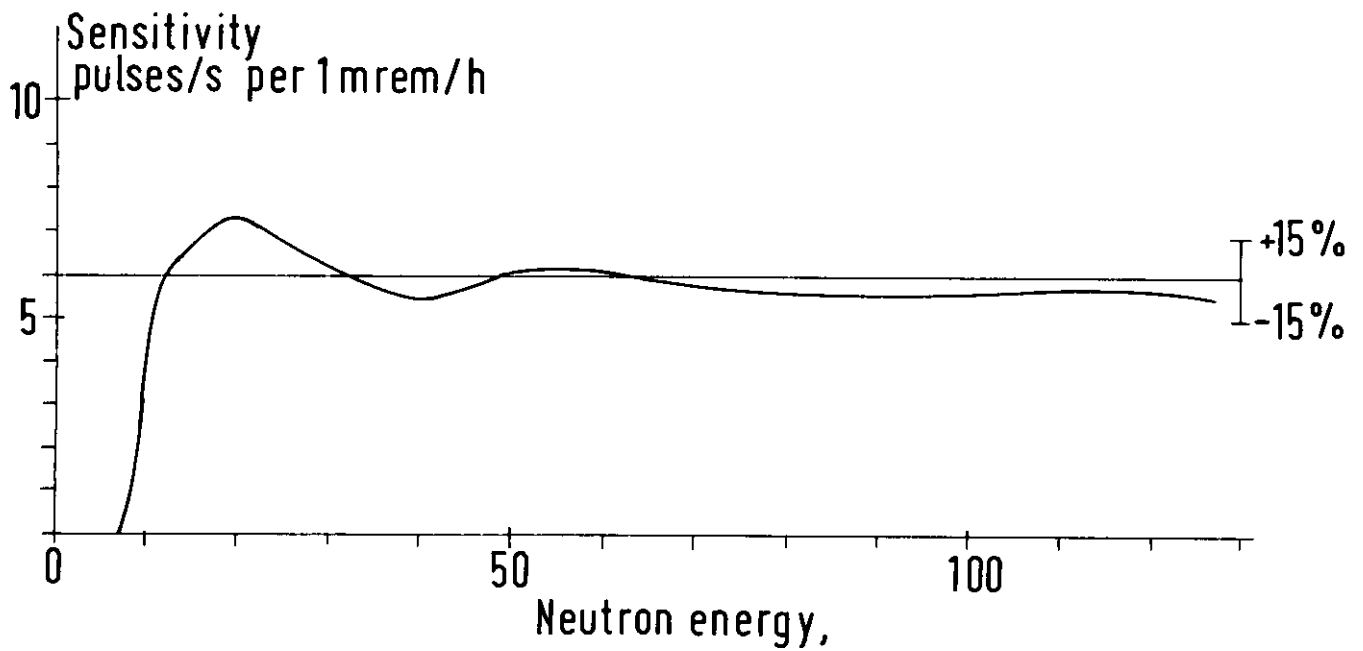


Fig. 7

